ON OPTIMAL SIGNALING SCHEMES OF 1-BIT ADC IN NON-COHERENT BLOCKAGE FADING

Mai T. P. Le[1]*, Minh N. Vu[2], Hung Nguyen-Le[3], Nghi H. Tran[4], Hieu V. Nguyen[1], Vien Nguyen-Duy-Nhat[1]

[1]The University of Danang - University of Science and Technology, Vietnam
[2]Independent Researcher, Vietnam
[3]The University of Danang - University of Technology and Education, Vietnam
[4]University of Akron, Akron, OH 44325, USA

*Corresponding author: lpmai@dut.udn.vn

(Received: May 02, 2025; Revised: June 14, 2025; Accepted: June 20, 2025)

DOI: 10.31130/ud-jst.2025.23(10B).645E

Abstract - Low-resolution analog-to-digital converters (ADCs), especially 1-bit quantizers, enable power- and cost-efficient wideband, large-scale MIMO. We study non-coherent fast-fading channels with probabilistic line-of-sight (LoS) blockage under 1-bit output quantization. The model randomly switches between Rayleigh (A = 0) and Rician (A = 1) fading, capturing environments where the LoS path intermittently appears. Without CSI at either end, we analyze mutual information and characterize the capacity-achieving input distribution. We prove that any optimal input exhibits π/2-rotational symmetry and derive necessary and sufficient Kuhn–Tucker conditions for optimality. Simulations show that the optimum tends to a four-point square constellation whose orientation aligns with the LoS phase when present. These results quantify the impact of probabilistic LoS on capacity and guide input design for energy-constrained, dynamically fading systems.

Key words - 1 bit ADC; blockage model; non-coherent channel; KTC; CSI.

1. Introduction

The increasing demand for high data rates in modern wireless communication systems - particularly in wideband and large-scale multiple-input multiple output (MIMO) deployments - has motivated extensive research into power efficient and cost-effective transceiver architectures [1, 2]. One promising direction is the use of low-resolution analog-to-digital converters (ADCs), especially the extreme case of 1-bit quantization, which significantly reduces power consumption and hardware complexity. These advantages make 1-bit ADCs particularly attractive for massive MIMO base stations and energy-constrained wireless devices [3]. However, the severe non-linearity induced by such coarse quantization poses major challenges in both system design and performance analysis, requiring new models and signaling strategies [4, 5].

Information-theoretic tools are critical for quantifying the performance limits of systems operating with quantized outputs [6,7]. Understanding channel capacity under various fading environments and quantization levels is essential for guiding the design of practical systems. Over the last decade, substantial information-theoretic progress has been made for systems using 1-bit and low-bit ADCs under various fading conditions [8]. For instance, in [9], the KKT conditions were examined and Dubin's theorem on extreme points of convex sets were used to address the detailed characteristics of optimal inputs for 1-bit ADCs in Rician fading. Rician model is general enough to represent small-scale fading in line-of-sight (LOS), non-line-of-sight (NLOS), as well as mmWave outdoor environment.

In this paper, we extend the study on capacity and optimal input signaling schemes of 1-bit ADC to a blockage fading channel, which plays a crucial role in mmWave communications [10]. The channel model captures probabilistic line-of-sight (LoS) blockage, encompassing both Rayleigh fading (non-LoS) and Rician fading (dominant LoS), thus reflecting the stochastic nature of wireless propagation in dynamic environments [10,11]. We adopt a non-coherent fast-fading setting with no channel state information (CSI) at either the transmitter or receiver - an assumption relevant to highly mobile scenarios or systems without CSI feedback [12].

The main contributions of this work can be listed as follows. First, we conduct a rigorous mutual information analysis of the mixed fading channel under 1-bit quantization and establish the existence and structure of the capacity achieving input distribution [13]. Interestingly, we find that the optimal input exhibits $\pi/2$ rotational symmetry - a pattern consistently observed in low resolution quantized systems [14]. Second, we derive necessary and sufficient conditions for input optimality using the Kuhn-Tucker conditions (KTC) framework [15], providing theoretical insight into signal design under non-linear constraints. Finally, we present extensive numerical simulations illustrating the geometry of the optimal input distribution. Results show a clear tendency toward a square-grid four-point constellation, whose orientation aligns with the LoS component when present, highlighting the significant impact of probabilistic LoS dynamics on both capacity and signal structure in energy-efficient wireless systems with 1-bit quantization [16].

The remainder of the paper is organized as follows. Section II presents the system model with the quantization and conditional probability functions. Section III investigates the mutual information formulation, while Section IV explores the structure of the optimal input and derives optimality conditions using KTC theory. Section V reports numerical results. Section VI concludes the paper.

2. System model

2.1. Channel Model

First, we verify the discrete memoryless channel framework as in [17], in which, the output is the unquantized received signal Z. Then, the output of 1-bit ADC Y is obtained by quantizing the received signal.

$$Z = A(mX) + GX + N \quad (1)$$

$$Y = Q(Z) \quad (2)$$

The symbol X represents a random variable with complex values, while m denotes a fixed complex-valued scaling factor. Both G and N are modeled as circularly symmetric complex Gaussian variables with zero mean, drawn independently and identically, and uncorrelated with the transmitted signal, with the corresponding variances $E\{|a|^2\} = \gamma^2$ and $E\{|n|^2\} = N_0$. In this work, we consider a mixed fading channel model with probabilistic line-of-sight (LoS) blockage, in which the model switches between Rayleigh fading (when A = 0) and Rician fading (when A = 1), capturing practical scenarios where the LoS path may appear or disappear randomly due to environmental dynamics. This is illustrated in Fig. 1, where the factor A is a Bernoulli random variable modeling blockage with probability of blockage p_B. The operator $Q(.)$ represents the low-resolution ADCs at the receiver and the quantized output is Y. The transmitted signal adheres to a power constraint, specifically ensuring that its average squared magnitude does not exceed a given threshold as such: $E\{|x|^2\} \leq P$.

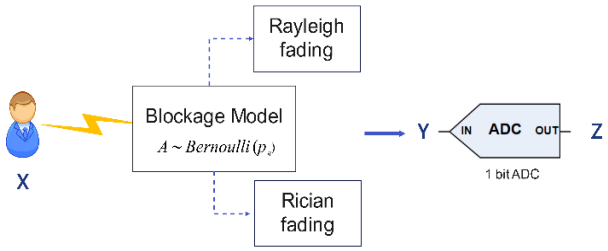

Figure 1. *The blockage model*

2.2. Quantization

The receiving signal Z is composed of in-phase and quadrature components, each quantized independently using identical 1-bit ADCs with zero thresholds. The real and imaginary outputs are denoted as Y_R and Y_I. Hence, the complex output Y can be expressed as,

$$Y = Y_R + jY_I = \text{sign}(Z_R) + j\text{sign}(Z_I) \quad (3)$$

Since this quantization is 1-bit ADC, Y has four distinct values $Y \in \{(1+j),(-1+j),(-1-j),(1-j)\}$. In this paper, we denote Y_c where $c \in \{R,I\}$ is the real or imaginary components of Y.

2.3. Conditional Probability Functions

When $X = x$ and $A = 1$, the variable Z follows a complex Gaussian distribution characterized by a mean of mx and variance $\sigma = \frac{1}{2}(\gamma^2|x|^2 + N_0)$, thus we have

$$p_Z^1 = p_{Z|A,X}(z|1,x) = \frac{1}{\pi(\gamma^2|x|^2+N_0)} e^{-\frac{|z-mx|^2}{\gamma^2|x|^2+N_0}}. \quad (4)$$

On the other hand, when $A = 0$, the distribution of Z remains complex Gaussian but with a zero mean and a modified variance $\sigma = \frac{1}{2}(\gamma^2|x|^2 + N_0)$,

$$p_Z^0 = p_{Z|A,X}(z|0,x) = \frac{1}{\pi(\gamma^2|x|^2+N_0)} e^{-\frac{|z|^2}{\gamma^2|x|^2+N_0}}. \quad (5)$$

As a result, the conditional distribution of Z when X is known can be described by the weighted combination as follows

$$p_{Z|X}(z|x) = p_B p_z^0 + (1-p_B)p_z^1. \quad (6)$$

It is possible to decouple the real and imaginary parts of the received signal R as

$$\begin{aligned} p_{Z|X}(z|x) &= \sqrt{\frac{p_B}{\pi(\gamma^2|x|^2+N_0)}} \exp\left(-\frac{z_R^2}{\pi(\gamma^2|x|^2+N_0)}\right) \\ &\times \sqrt{\frac{p_B}{\pi(\gamma^2|x|^2+N_0)}} \exp\left(-\frac{z_I^2}{\pi(\gamma^2|x|^2+N_0)}\right) \\ &+ \sqrt{\frac{1-p_B}{\pi(\gamma^2|x|^2+N_0)}} \exp\left(-\frac{z_R^2}{\pi(\gamma^2|x|^2+N_0)}\right) \\ &\times \sqrt{\frac{1-p_B}{\pi(\gamma^2|x|^2+N_0)}} \exp\left(-\frac{z_I^2}{\pi(\gamma^2|x|^2+N_0)}\right) \\ &= p_B p_{z_R}^0 p_{z_I}^0 + (1-p_B)p_{z_R}^1 p_{z_I}^1 \end{aligned} \quad (7)$$

Since the output signal y in 1-bit quantized channel is circular symmetry, we can examine one quadrant and generalize the results for other quadrants in the complex plane. By considering the positive quadrant $y_1 = 1 + j$ we have the probability $Y = y_1$ given $X = x$ is

$$\begin{aligned} p_{Y|X}(y_1|x) &= \int_{z\in Q_1} p_{Z|X}(z|x)\,dz \\ &= \int_{z_R\geq 0}\int_{z_I\geq 0} p_B p_{z_R}^0 p_{z_I}^0 + (1-p_B)p_{z_R}^1 p_{z_I}^1 dz_R dz_I \\ &= \frac{p_B}{4} + (1-p_B)Q\left(-\frac{\sqrt{2}(-m_R x_R + m_I x_I)}{\sqrt{\gamma^2|x|^2+N_0}}\right) \\ &\times Q\left(-\frac{\sqrt{2}(-m_R x_R - m_I x_I)}{\sqrt{\gamma^2|x|^2+N_0}}\right). \end{aligned} \quad (8)$$

Here $Q(x)$ denotes the standard complementary Gaussian function, defined by the integral $Q(\frac{1}{\sqrt{2\pi}}\int_x^\infty \exp(-\frac{u^2}{2})\,du$ is the well-known complementary Gaussian distribution function, which is a widely recognized function in probability theory and communications, commonly called the Q−function. Now, let denote

$$x_1 = \frac{-m_R x_R + m_I x_I}{|m|} \quad (9)$$

$$x_2 = \frac{-m_R x_R - m_I x_I}{|m|} \quad (10)$$

Notice that $x_1^2 + x_2^2 = |x|^2$. Substituting back to (9) we obtain

$$\begin{aligned} &p_{Y|X}(y_1|x) \\ &= \frac{p_B}{4} + (1-p_B)Q\left(\frac{\sqrt{2}|m|x_1}{\gamma^2|x|^2+N_0}\right)Q\left(\frac{\sqrt{2}|m|x_2}{\gamma^2|x|^2+N_0}\right) \end{aligned} \quad (11)$$

For simplicity, we denote $W_i = p_{Y|X}(y_i|x)$ for

$i \in \{1,2,3,4\}$. The conditional probabilities for $2 \le i \le 4$ can also be derived using the same approach as

$$W_i = \frac{p_B}{4} + (1-p_B)Q\left(\frac{\sqrt{2}|m|x_1}{\gamma^2|x|^2+N_0}\right) Q\left(\frac{\sqrt{2}|m|x_2}{\gamma^2|x|^2+N_0}\right). \quad (12)$$

From (12), it is straightforward that

$$W_i(x) = W_{i+1}(xe^{j\pi/2}), \quad (13)$$

where $W_{i+1}(x) = W_1(x)$ if $i = 4$. (13) then results in the following expression

$$\sum_{i=1}^{4} W_i(x) log W\_i(x) = \sum_{i=1}^{4} W_i\left(xe^{\frac{i\pi}{2}}\right) log W_i(xe^{\frac{i\pi}{2}}) \quad (14)$$

3. Mutual information and Channel capacity

First, we assume an input random variable X with a distribution represented by $F_X(x)$. For simplicity, we will use $F_X(x)$and F_X interchangeably to refer to this distribution throughout the work. The mutual information between X and Y, denoted as $I(X;Y) = I(F_X)$ and expressed as a function of the input distribution F_X is defined by the integral below.

$$I(F_X) = \int_C \sum_{i=1}^{4} p(y_i|x) \log \frac{p(y_i|x)}{p(y_i;F_X)}\, dF_X(x). \quad (15)$$

Alternatively, mutual information can be expressed as the difference between the output entropy and the conditional entropy:

$$I(X;Y) = I(F_X) = H_{F_X}(Y) - H_{F_X}(Y|X). \quad (16)$$

Then, the output entropy $H_F(Y)$ is defined by the following integral expression:

$$H_{F_X}(Y) = -\int_C \sum_{i=1}^{4} W_i(x) log p(y_i|x)\, dF_X(x) \quad (17)$$

Moreover, the conditional entropy term $H_{F_X}(Y|X)$ in eq. (16) can be written as:

$$H_{F_X}(Y|X) = -\int_C \sum_{i=1}^{4} W_i(x) log W_i(x)\, dF_X(x) \quad (18)$$

where the output probability $p(y_i;F_X)$, $1 \le i \le 4$, is

$$p(y_i|F_X) = \int_C W_i(x)\, dF_X(x). \quad (19)$$

Channel capacity C is defined as the maximum achievable mutual information across all input distributions that meet the given power constraint (2). Let Ω denote the set of all valid input distributions for X that satisfy the power constraint. Then, the channel capacity is expressed as:

$$C = sup I(F_X). \quad (20)$$

4. Characterization of the Optimal Input Distribution

4.1. Existence and Symmetry of Optimal Inputs

Theorem 1: Given any input distribution F_X^1, we can construct a new distribution F_X defined by:

$$F_X = \frac{1}{4}\left(F_X^1(x) + F_X^1\left(xe^{j\pi/2}\right) + F_X^1(xe^{j\pi}) + F_X^1\left(xe^{j3\pi/2}\right)\right) \quad (21)$$

This new distribution is $\pi/2$ − rotationally symmetric and preserves the same conditional entropy circular symmetric distribution $H_{F_X}(Y|X)$, while increasing or maximizing the output entropy $H_{F_X}(Y|X)$.

Proof: From (18), the conditional entropy when the input distribution is F_X can be calculated as,

$$\begin{aligned}
H_F(Y|X) &= -\int_C \sum_{i=1}^{4} W_i(x) log W_i(x)\, dF_X(x) \\
&= -\int_C \sum_{i=1}^{4} \frac{1}{4} W_i(x) log W_i(x) \\
&\quad \times d(F_X^1(x) + F_X^1(xe^{j\pi/2}) + F_X^1(xe^{j\pi}) + F_X^1(xe^{j3\pi/2}) \\
&= -\frac{1}{4}\int_C \sum_{i=1}^{4} W_i(x) log W_i(x)\, dF_X^1(x) \\
&\quad -\frac{1}{4}\int_C \sum_{i=1}^{4} W_i(xe^{j\pi/2}) log W_i(xe^{j\pi/2})\, dF_X^1(xe^{j\pi/2}) \\
&\quad -\frac{1}{4}\int_C \sum_{i=1}^{4} W_i(xe^{j\pi}) log W_i(xe^{j\pi})\, dF_X^1(xe^{j\pi}) \\
&\quad -\frac{1}{4}\int_C \sum_{i=1}^{4} W_i(xe^{j3\pi/2}) log W_i(xe^{j3\pi/2})\, dF_X^1(xe^{j3\pi/2})
\end{aligned} \quad (22)$$

Next, utilize F_X, we have:

$$\begin{aligned}
p(y_1|F_X) &= \int_C W_1(x)\, dF_X(x) \\
&= \frac{1}{4}\int_C W_1(x)\, dF_X^1(x) + \frac{1}{4}\int_C W_1(x)\, dF_X^1(xe^{j\pi/2}) \\
&\quad + \frac{1}{4}\int_C W_1(x)\, dF_X^1(xe^{j\pi}) + \frac{1}{4}\int_C W_1(x)\, dF_X^1(xe^{j3\pi/2}) \\
&= \frac{1}{4}\int_C W_1(x)\, dF_X^1(x) + \frac{1}{4}\int_C W_2(x)\, dF_X^1(x) \\
&\quad + \frac{1}{4}\int_C W_3(x)\, dF_X^1(x) + \frac{1}{4}\int_C W_4(x)\, dF_X^1(x) \\
&= \frac{1}{4}\int_C dF_X^1(x) = \frac{1}{4}
\end{aligned} \quad (23)$$

Since the output distribution is uniform, it follows that F_X achieves the maximum possible output entropy. Based on Theorem 1, we can restrict our attention to circularly symmetric input distributions F_X in Ω, as they suffice for optimality. The mutual information for circular symmetric input can be written as:

$$\begin{aligned}
I(F_X) &= log(4) - H_{F_X}(Y|X) \\
&= log(4) + \int_C \sum_{i=1}^{4} W_i(x) log W_i(x)\, dF_X(x).
\end{aligned} \quad (24)$$

4.2. The Kuhn-Tucker Condition (KTC)

This section aims to derive the KTC, a necessary and sufficient criterion for determining when a circularly symmetric input distribution is optimal.

Lemma 1. *A distribution F_X satisfies the power constraint P and is optimal if and only if there exists a non-negative $\mu \ge 0$ such that*

$$\sum_{i=1}^{4} W_i(x) log W_i(x) - \mu(|x|^2 - P) + log(4) - C \le 0, \forall x \in \mathbb{C}. \quad (25)$$

Equality occurs when x lies within the support of the optimal distribution F_X.

4.3. Phase of mass points of Optimal input

In order to examine the phase of mass points of optimal input, we fix the mass points' amplitude and analyze the

phase by Lagrange multiplier.

Denote F^*_X is an optimal solution. Given that $P > 0$, at least one mass point $x^* \in supp(F^*_X)$ that satisfies $|x^*|^2 > 0$ $|x^*| > 0$. Applying the KTC, it achieves

$$-\sum_{i=1}^{4} W_i(x^*) log W_i(x^*) + \mu(|x^*|^2 - P) + \mathrm{C} - \log(4) = 0, \quad (26)$$

Denoting $A = |x^*|^2$ and the set $\mathrm{S_A}$ containing all pair of points $(\mathrm{x_1}, \mathrm{x_2}) \in \mathbb{R}^2$ such that $\mathrm{x_1^2} + \mathrm{x_2^2} = \mathrm{A}$. We further define function $\mathrm{K}(\mathrm{x_1}, \mathrm{x_2})$ on $\mathrm{S_A}$ as follows

$$\mathrm{K}(\mathrm{x_1}, \mathrm{x_2}) = -\sum_{i=1}^{4} W_i(\mathrm{x_1^*}, \mathrm{x_2^*}) log W_i(\mathrm{x_1^*}, \mathrm{x_2^*}) + \mu(\mathrm{A} - P) + \mathrm{C} - \log(4) \quad (27)$$

From the KTC, we have

$$\mathrm{K}(\mathrm{x_1}, \mathrm{x_2}) \geq 0, \forall x \in S_A \quad (28)$$

$$\mathrm{K}(\mathrm{x^*}_1, \mathrm{x^*}_2) = 0 \quad (29)$$

Therefore,

$$(\mathrm{x_1^*}, \mathrm{x_2^*}) = \arg min_{(x_1, x_2) \in A} = \textstyle\sum_{i=1}^{4} W_i(\mathrm{x_1^*}, \mathrm{x_2^*}) log W_i(\mathrm{x_1^*}, \mathrm{x_2^*}) \quad (30)$$

The constraint $(x_1, x_2) \in S_A$ is equivalent to $\mathrm{x_1^2} + \mathrm{x_2^2} = \mathrm{A}$. Hence, we have the Lagrangian

$$L(\mathrm{x_1}, \mathrm{x_2}, \lambda) = -\sum_{i=1}^{4} W_i(\mathrm{x_1^*}, \mathrm{x_2^*}) log W_i(\mathrm{x_1^*}, \mathrm{x_2^*}) + \lambda(\mathrm{x_1^2} + \mathrm{x_2^2} - \mathrm{A}) \quad (31)$$

For simplicity, we denote $\beta = \frac{\sqrt{2}|m|}{\sqrt{\gamma^2 \mathrm{A} + \mathrm{N_0}}}$. For $(\mathrm{x_1^*}, \mathrm{x_2^*})$ to qualify as a minimizer, the following condition must hold:

$$\nabla_{\mathrm{x_1}} L(\mathrm{x_1}, \mathrm{x_2}, \lambda) = 0 \quad (32)$$

$$\nabla_{\mathrm{x_2}} L(\mathrm{x_1}, \mathrm{x_2}, \lambda) = 0, \quad (33)$$

which is equivalent to

$$2\lambda \mathrm{x_1} - (1 - p_B)\beta \frac{e^{-\beta^2 \mathrm{x_1^2}/2}}{\sqrt{2\pi}} \left[Q(\beta x_2) log \left(\frac{\frac{p_B}{4} + (1-p_B) Q(-\beta x_1) Q(\beta x_2)}{\frac{p_B}{4} + (1-p_B) Q(\beta x_1) Q(\beta x_2)} \right) + Q(-\beta x_2) log \left(\frac{\frac{p_B}{4} + (1-p_B) Q(-\beta x_1) Q(-\beta x_2)}{\frac{p_B}{4} + (1-p_B) Q(\beta x_1) Q(-\beta x_2)} \right) \right] = 0, \quad (34)$$

$$2\lambda \mathrm{x_2} - (1 - p_B)\beta \frac{e^{-\beta^2 \mathrm{x_2^2}/2}}{\sqrt{2\pi}} \left[Q(\beta x_1) log \left(\frac{\frac{p_B}{4} + (1-p_B) Q(-\beta x_2) Q(\beta x_1)}{\frac{p_B}{4} + (1-p_B) Q(\beta x_2) Q(\beta x_1)} \right) + Q(-\beta x_1) log \left(\frac{\frac{p_B}{4} + (1-p_B) Q(-\beta x_2) Q(-\beta x_1)}{\frac{p_B}{4} + (1-p_B) Q(\beta x_2) Q(-\beta x_1)} \right) \right] = 0. \quad (35)$$

Solving the eqs. (34-35) shall help us identify the phase property, and as a result, the exact location of the optimal mass points. While the analytical solution of the phases is beyond the scope of this work, we believe that the approach in [9] can be used to find the exact phases. Instead, in the following, as an illustrative example, we shall rely on numerical search using the KTC to obtain these phases and validate them using (34-35).

5. Numerical results

In this section, we resort to a numerical method to validate the theoretical analysis concerning capacity-achieving input distributions for 1-bit quantized non-coherent blockage fading channels, with probability of blockage $p_B = 0.2$. Note that to obtain the optimal signals, we can use a traditional gradient descent-based method to search for the optimal input and verify it with the KTC. As an alternative, eqs. (34-35) can be used to search and validate the optimal phases of the optimal rotated QPSK signal.

In Figure 2, we plot the KTC at SNR = 1 dB. It can be seen that the KTC surface exhibits a smooth, symmetric shape with four clear optimal points forming a square constellation aligned with the LoS phase. These four phases can be verified to be the solutions of (34) and (35). This confirms that even under high noise, the capacity achieving input maintains $\pi/2$-rotational symmetry, validating the robustness of the analytically derived rotated QPSK structure.

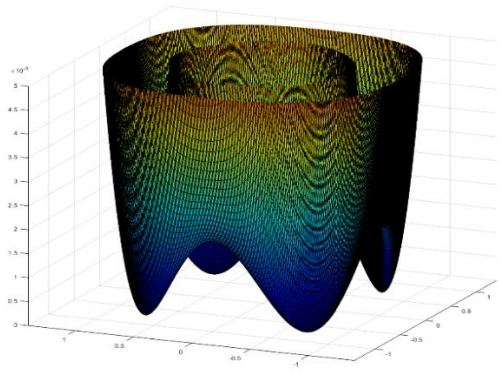

Figure 2. *The KTC with SNR = 1*

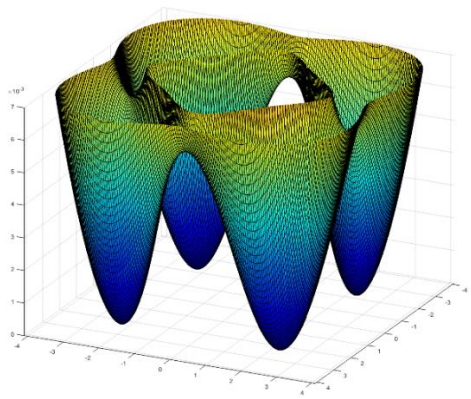

Figure 3. *The KTC with SNR= 10*

Figure 3 reveals sharper and more structured KTC surfaces at SNR = 10 dB, reflecting the stronger influence of the deterministic LoS component and the need for precise constellation alignment. The optimal points become more concentrated, clearly demonstrating that the rotation angle of the four-point input must match the LoS phase to maximize mutual information.

Together, Figures 2 and 3 confirm that the optimal input reduces to a rotated QPSK constellation with four equally powered mass points placed on a square grid, aligned with the LoS direction. This structure, derived analytically through KTC analysis and the Gaussian Q-function, adapts to channel conditions without requiring CSI, making it well-suited for practical low-resolution MIMO systems such as those in mmWave applications.

In the end, these results reinforce the theoretical basis for phase-aligned rotated QPSK as the optimal signaling strategy in 1-bit quantized non-coherent Rician fading channels.

6. Conclusions

This paper investigated the capacity and input design of 1-bit quantized, noncoherent wireless systems over a blockage-mixed Rician and Rayleigh fading channel. We demonstrated that the capacity-achieving input is a rotated QPSK constellation with $\pi/2$-rotational symmetry, optimally aligned with the LoS phase when present. Both theoretical analysis and simulations confirm the robustness and efficiency of this design, offering practical insights for energyconstrained systems without CSI.

Acknowledgments: The work by Hung Nguyen-Le and Mai T. P. Le was supported by the Ministry of Education and Training under Project B2024.DNA.13.

REFERENCES

[1] E. G. Larsson, O. Edfors, F. Tufvesson, and T. L. Marzetta, "Massive MIMO for Next Generation Wireless Systems", *IEEE Commun. Mag.,* vol. 52, no. 2, pp. 186–195, 2014.

[2] M. T. P. Le, H. V. Nguyen, V. Nguyen-Duy-Nhat, and L. Sanguinetti, "QoE-aware power allocation for aerial-relay massive MIMO networks," *IEEE Transactions on Network and Service Management*, vol. 21, no. 1, pp. 477–489, 2023.

[3] S. Han, C.-L. I, Z. Xu, C. Rowell, and L. Hanzo, "Large-Scale Antenna Systems With Hybrid Analog and Digital Beamforming for 5G Millimeter Wave Communications", *IEEE Commun. Mag*., vol. 53, no. 1, pp. 186–194, 2015.

[4] M. T. P. Le, V. Nguyen-Duy-Nhat, H. V. Nguyen, and O.-S. Shin, "DDPG-based optimization for zero-forcing transmission in UAV-relay massive MIMO networks," *IEEE Open Journal of the Communications Society*, vol. 5, pp. 2319–2332, 2024.

[5] A. Mezghani and J. A. Nossek, "Capacity Analysis of Rayleigh-Fading Channels With 1-Bit Quantized Output", *in Proc. IEEE Int. Symp. Inf. Theory (ISIT)*, 2008, pp. 2303–2307.

[6] T. M. Cover and J. A. Thomas, *Elements of Information Theory*. Wiley, 2 ed., 2006.

[7] C. E. Shannon, "A Mathematical Theory of Communication", *Bell Syst. Tech. J.*, vol. 27, no. 3, pp. 379–423, 1948.

[8] A. Alkhateeb, G. Leus, and R. W. H. Jr., "MIMO Communications With Finite-Resolution Quantization", *IEEE Trans. Inf. Theory*, vol. 61, no. 6, pp. 2847–2868, 2015.

[9] M.N. Vu, N.H. Tran, D.G. Wijeratne, K. Pham, K.S. Lee, and D.H. Nguyen, Optimal signaling schemes and capacity of non-coherent Rician fading channels with low-resolution output quantization. *IEEE Transactions on Wireless Communications*, vol. 18, no. 6, pp. 2989-3004, 2019.

[10] D. Kumar, J. Kaleva, and A. Tölli, Blockage-aware reliable mmWave access via coordinated multi-point connectivity. *IEEE Transactions on Wireless Communications*, vol. 20, no. 7, pp.4238-4252. 2021.

[11] S. Loyka, "Channel Capacity of MIMO Architecture With Probabilistic Line-of-Sight", *IEEE Trans. Wireless Commun.*, vol. 9, no. 7, pp. 2246– 2256, 2010.

[12] I. C. Abou-Faycal, M. D. Trott, and S. S. (Shitz), "The Capacity of Discrete-Time Memoryless Rayleigh-Fading Channels", *IEEE Trans. Inf. Theory*, vol. 47, no. 4, pp. 1290–1301, 2001.

[13] J. Yang, S. Zhou, X. Wang, and H. V. Poor, "On the Capacity-Achieving Input of Channels With Phase Quantization", *IEEE Trans. Inf. Theory*, vol. 68, no. 8, pp. 5063–5078, 2022.

[14] L. You and W. Yu, "Achievable Rate of 1-Bit Quantized Massive MIMO Uplink With Pilot Contamination", *IEEE Trans. Commun.*, vol. 64, no. 12, pp. 5197–5211, 2016.

[15] S. Boyd and L. Vandenberghe, *Convex Optimization*. Cambridge Univ. Press, 2004.

[16] Y. Zhang, P. Wang, Q. Li, L. Yang, and C. Han, "Enhanced Signal Detection and Constellation Design for Massive SIMO Communications With 1-Bit ADCs", *Wireless Commun. Mob. Comput.*, vol. 2023, pp. 1–11, 2023.

[17] M. C. Gursoy, H. V. Poor, and S. Verdú, "The noncoherent Rician fading channel-Part I: Structure of the capacity-achieving input," *IEEE Transactions on Wireless Communications*, vol. 4, no. 5, pp. 2193–2206, 2005.